Templated Self-Assembly and Local Doping of Molecules on Epitaxial Hexagonal Boron Nitride

Fabian Schulz, Robert Drost, Sampsa K. Hämäläinen, and Peter Liljeroth*

Department of Applied Physics, Aalto University School of Science, P.O. Box 15100, 00076 Aalto, Finland

ABSTRACT Using low-temperature scanning tunneling microscopy, we show that monolayer hexagonal boron nitride (h-BN) on Ir(111) acts as ultrathin insulating layer for organic molecules, while simultaneously templating their self-assembly. Tunneling spectroscopy experiments on cobalt phthalocyanine (CoPC) reveal narrow molecular resonances and indicate that the charge state of CoPC is periodically modulated by the h-BN moiré superstructure. Molecules in the second layer show site-selective adsorption behavior, allowing the synthesis of molecular dimers that are spatially ordered and inaccessible by usual chemical means.

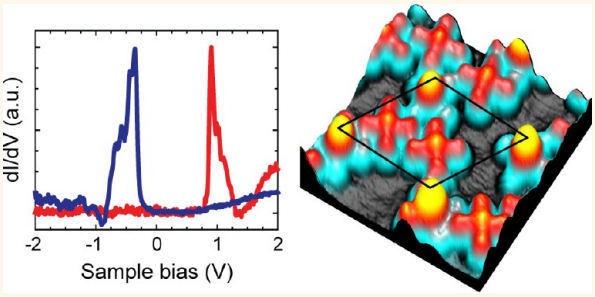

KEYWORDS: cobalt phthalocyanine (CoPC) · hexagonal boron nitride · scanning tunneling microscopy · local doping · molecular resonances · ultrathin insulating layer

Since the discovery of the boron nitride nanomesh,[1] ultrathin layers of hexagonal boron nitride (h-BN) have been praised as a versatile nanotemplate for future molecular electronic devices.[2−6] The "nanomesh" is a manifestation of the moiré superstructure caused by the lattice-mismatch between the h-BN and the underlying Rh(111) substrate. As the registry of B and N atoms with respect to the substrate atoms is modulated, a periodic pattern of strongly interacting "pores" separated by weakly interacting "wires" is formed. The stereotypical h-BN nanomeshes on Rh(111) or Ru(0001) exhibit strong moiré corrugation (*ca.* 1−1.5 Å) and work function modulation (the difference between the pore and the wire is *ca.* 0.5 eV).[7]

The properties of the h-BN moiré can be tuned by changing the metal support. In particular, the symmetry of the superstructure and its periodicity is altered by the crystal orientation[2,8] and the lattice constant[3,9,10] of the metal substrate, respectively. The electronic properties of the h-BN layer depend strongly on the substrate as well. While bulk h-BN is a wide-band gap insulator,[11,12] there is theoretical and experimental evidence that on strongly interacting substrates such as Ni(111), Rh(111) and Ru(0001), h-BN exhibits metallic character.[7,13−15] On the other hand, there are STM experiments on probing the size-dependent superconductivity of small metallic particles and spin-excitations in Mn_{12} molecular magnets, where h-BN on Rh(111) was used as a decoupling layer.[16,17] Finally, on the much more weakly interacting Cu(111) substrate, the h-BN monolayer has been shown to keep its insulating properties.[6]

Ultrathin insulating layers supported by metal substrates (*e.g.*, oxides, alkalihalides) have attracted increasing interest in recent years as they are able to host eletronic states decoupled from the metallic surface.[18−24] In particular, it is feasible to investigate electronic states and electron-vibration coupling in molecular systems essentially unperturbed by the metal support.[21,23−25] In some specific cases, it is even possible to observe molecules in multiple charge states and switch between them.[26−28] A system combining the templating capabilities of a moiré superstructure with the decoupling properties of ultrathin insulating layers would be of particular value to fundamental research as well as for future molecular electronic devices. The strong geometric corrugation together with the work function modulation on the h-BN nanomesh has been shown to allow confining molecules spatially to the pores of the moiré

* Address correspondence to peter.liljeroth@aalto.fi.

Received for review September 16, 2013 and accepted October 23, 2013.

Published online October 23, 2013
10.1021/nn404840h

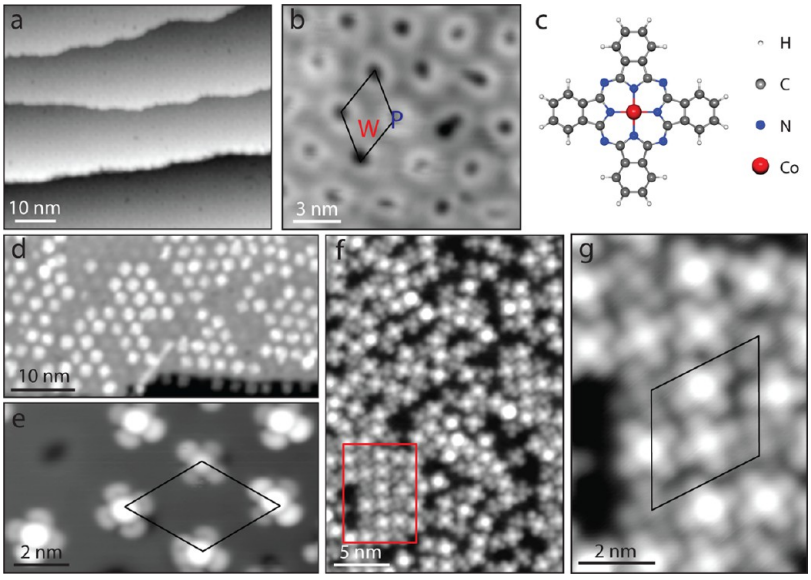

Figure 1. Self-assembly of CoPC on hexagonal boron nitride on Ir(111). (a and b) Overview (a) and zoomed-in (b) images of the clean h-BN/Ir(111) surface. W and P denote the wire and pore regions of the moiré unit cell, respectively. (c) Model of CoPC. (d and e) Self-assembly in the low coverage regime with one molecule per moiré unit cell. (f and g) Larger coverage results in filling the wires with locally square-packed regions. The image in panel g corresponds to the area marked by the red rectangle in panel f. The moiré unit cell is marked by a black parallelogram in panels b, e, and g. Feedback parameters: (a and b) −0.484 V, 527 pA; (d) 1.738 V, 12 pA; (e) −2.029 V, 39 pA; (f) 0.484 V, 20 pA; (g) 0.484 V, 48 pA.

superstructure, demonstrating the capability of h-BN monolayers to guide the growth of nanostructures.[4,5,29] However, experiments unraveling the degree of electronic coupling of molecular states and the underlying metal substrate have not been carried out previously.

Using scanning tunneling microscopy (STM) and spectroscopy (STS), we show for the first time that monolayer h-BN can indeed act as an ultrathin insulating layer for adsorbed molecules while simultaneously templating their self-assembly. At low coverages, cobalt phthalocyanine (CoPC) molecules evaporated onto h-BN on Ir(111)[30] selectively adsorb only on the pores of the moiré superstructure, while at larger coverages locally square-packed ordered islands emerge. Differential conductance spectroscopy (d*I*/d*V*) shows molecular resonances with a very narrow line width, which is modulated by the adsorption site. The charge state of the molecule is modulated by the moiré as well, leading to a local and periodic doping of the molecular layer. Finally, CoPC coverages above one monolayer result in formation of CoPC dimers in the pore regions of the moiré unit cell.

RESULTS AND DISCUSSION

Figure 1a is an STM overview image of h-BN grown on Ir(111) and shows a single h-BN domain extending over several terraces and monatomic steps, demonstrating the high quality of the film. The moiré superstructure arising due to the lattice mismatch between the Ir(111) surface and the h-BN layer is seen in more detail in the small-scale image in Figure 1b. The superstructure is formed by depressions arranged in a hexagonal lattice with a periodicity of ∼3 nm. The bright rim visible around the depression is an electronic effect and appears only at low bias. The electronic structure of the h-BN/Ir(111) system as well as the atomic registry of B and N atoms with respect to the Ir(111) lattice causing the moiré have been studied in detail by a combination of STM experiments and DFT calculations in another work.[31] The corrugation of the superstructure is ∼0.4 Å, indicating a weak interaction of the h-BN layer with the Ir(111) substrate (on Rh(111) and Ru(0001) the corrugation is around 1 Å). In the following, we use the usual terminology in describing the different areas of the moiré unit cell: the depressions of the moiré will be referred to as *pores*, while the surrounding areas will be referred to as *wires*.

At low coverages of CoPC well below one monolayer (ML), the molecules exclusively adsorb on the pores of the moiré to self-assemble into an array of perfect hexagonal symmetry, as demonstrated in Figure 1c. In this arrangement, each moiré unit cell is occupied by exactly one molecule, trapped on the pore. Such a behavior has been observed previously[4,5,29] and proves the ability of the h-BN moiré superstructure to serve as a nanotemplate for the bottom-up growth of artificial nanostructures. The zoom-in STM image in Figure 1e reveals an interesting detail: a significant fraction of the CoPC molecules is not adsorbed exactly in the center of the pore. The work function within the h-BN/Ir(111) moiré unit cell varies by ∼0.4 eV.[31] The largest work function gradient exists at the edge between pores and wire, leading to an electric field of the order of 0.1 V/nm. This large electric field can strongly influence the exact adsorption site of the molecule, *i.e.*, favoring an off-center position with respect to the center of the pore.[5]

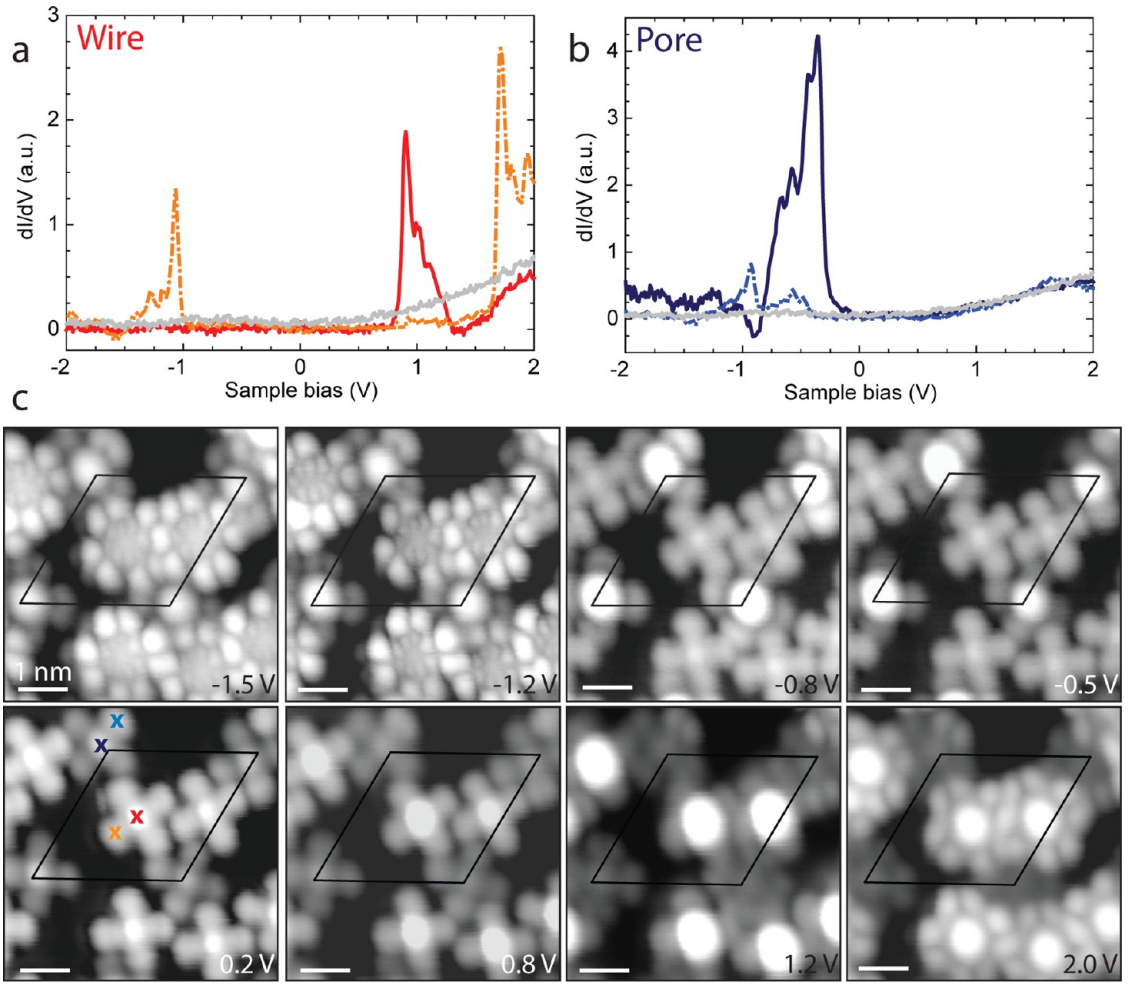

Figure 2. Differential conductance spectroscopy on CoPC on h-BN/Ir(111). (a) Spectra measured on the CoPC adsorbed in the wire region of the moiré unit cell; red solid line is measured on the metal center and orange dashed line on the carbon backbone (as indicated in the STM scan at 0.2 V in panel c). (b) Spectra measured on a molecule adsorbed in the pore region of the moiré unit cell; dark blue solid line is the metal center and light blue dashed the carbon backbone. The gray lines in panels a and b are reference spectra taken on clean h-BN. All spectra shown are taken with the same microscopic tip. (c) Series of STM images at different biases showing the various orbitals corresponding to the peaks in the d*I*/d*V* measurements. Set point current is 11 pA for all images.

Regimes of higher molecule coverages have been largely unexplored in the literature so far but might offer new ways to modulate the electronic properties of the adsorbates. Figure 1f shows the h-BN/Ir(111) substrate at a much higher CoPC coverage. Once all the pores of the moiré are occupied, the molecules start to assemble on the wires, forming locally square packed regions. This is demonstrated by the zoomed-in STM image shown in Figure 1g. We observe no long-range order neither directly after evaporation nor after annealing the sample up to 200 °C.

More careful investigation of Figure 1g shows that not all molecules appear the same. Two distinct molecular contrasts can be observed: the main difference is that the cobalt center appears either as a bright protrusion or not. In fact, the two distinct contrasts can be unambiguously matched to the molecule being adsorbed either on the pore or on the wire, indicating that the h-BN/Ir(111) moiré superstructure alters the electronic properties of adsorbed molecules in an ordered fashion.

To investigate the electronic properties of the two kinds of molecules more closely, we measured differential conductance spectra on the molecules. The electronic structure of CoPC on various metal substrates has been thoroughly studied using both normal and spin-polarized STM.[32−37] The measured d*I*/d*V* signal is proportional to the local density of states (LDOS). Panels a and b of Figure 2 compare the d*I*/d*V* spectra for CoPC adsorbed on the wire and on the pore, respectively. On the wire, the molecule exhibits a sharp resonance around 0.8 V located solely at the cobalt metal center. Two additional resonances at around 1.7 and −1.1 V are delocalized over the π system of the carbon backbone of the molecule. The resonance at 0.8 V on the central ion thus represents the lowest unoccupied molecular orbital (LUMO) of the wire CoPC. In stark contrast, molecules adsorbed on the pore do not

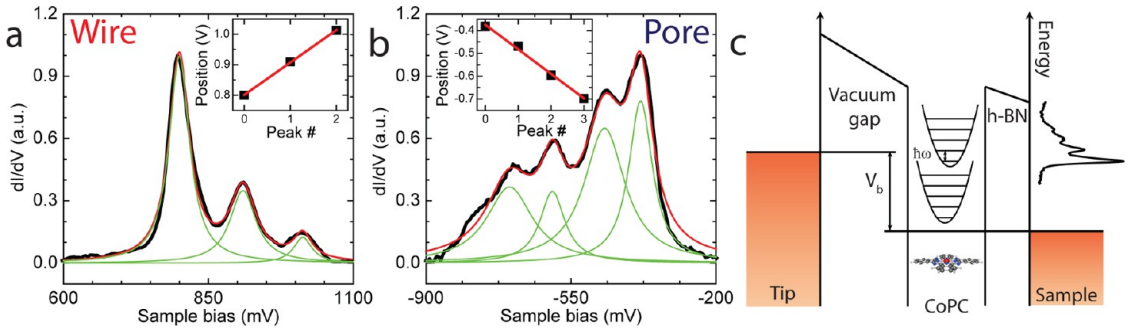

Figure 3. High resolution spectroscopy of the vibronic progressions. (a) LUMO of the CoPC adsorbed on the wire fitted with a sum of three Lorentzians (red line). The individual peaks are extracted from the fit parameters and plotted in green. (b) Analogously, the HOMO of the pore molecule fitted by four Lorentzians. In both panels a and b, the insets show a linear fit to the peak energies of the vibronic progression ('0' denotes the elastic peak, '1' the first vibronic replica, and so on). (c) Model of the double barrier tunneling junction formed by the STM and the CoPC adsorbed on the h-BN layer.

show any notable features at positive sample bias. However, a very prominent peak at around −0.4 V is found on the metal center, representing the CoPC's highest occupied molecular orbital (HOMO) when adsorbed on the pore of the h-BN moiré. It is worth noting that the gross features of the d*I*/d*V* spectra are highly reproducible within the group of wire or pore molecules. The exact energetic position of the peaks does vary by up to 200 mV within either group due to the work function changes within the different regions in the moiré unit cell[31] and, possibly, differences in the atomic registry between the molecule and the h-BN. Nevertheless, the number of resonances located at the metal center and at the carbon backbone and their order in energy as shown in Figure 2a,b is representative for the CoPC on h-BN/Ir(111) system.

Figure 2c displays a series of STM images taken at different biases. At low positive bias (0.2 V), where none of the spectra show considerable density of states, molecules on the wire and on the pore appear alike, resembling mostly the cross-shape of their carbon backbone. Increasing the sample bias (0.8 and 1.2 V) causes the metal center of the wire molecules to light up as the energy is in resonance with the LUMO. When the bias is further increased (2.0 V), the metal center becomes less bright again but the carbon backbone shows up more prominently, revealing the lobes of a delocalized π-orbital in accordance with the point spectroscopy shown in Figure 2a. Switching to negative sample bias (−0.5 and −0.8 V), the metal center of the pore CoPC lights up, showing its HOMO as expected from the d*I*/d*V* spectra (Figure 2b). At higher negative bias (−1.2 and −1.5 V) also the carbon backbone of the wire molecules developes distinct lobes as its first resonance below the Fermi level is reached.

The molecular resonances of CoPC adsorbed on the wire appear very similar to the case of CoPC deposited on graphene on an insulating substrate.[38] The situation on the pore is distinctly different. It is evident based on the STM imaging that the HOMO of the pore molecule and the LUMO of the wire molecule represent the same orbital, shifted by *ca.* 1.1 V to lower energies from the wire to the pore. Shifting the orbital below the Fermi level on the pore implies that is has become filled and thus, the CoPC is charged upon adsorption in the pore region of the h-BN moiré. Charging of molecules and atoms upon changing the substrate work function has been observed before on, for example, ultrathin NaCl layers on different copper single crystals.[28,39]

This effect is never observed for molecules adsorbed on the wire and therefore demonstrates a way for strongly localized doping of molecular thin films in an ordered fashion. The situation corresponds to an extremely high doping density of 1 charge per moiré unit cell, *i.e.*, $>10^{13}$ cm^{-2}. From the energy shift of the orbital of ∼−1.1 eV together with the increase of the work function from the pore to the wire of up to 0.4 eV, we can give a rough estimation of the charging energy of about 0.7−0.9 eV,[40] similar to the values reported for other phthalocyanines on NaCl ultrathin insulating film on Cu(100).[28]

The resonances in the d*I*/d*V* spectra (Figure 2a,b) not only are narrow, but also show vibronic satellite peaks due to inelastic tunneling. This is further evidence that the h-BN film acts as an insulating layer that decouples the molecules from the metallic substrate.[25] The vibronic features arise as an electron that is injected into a molecule at an excess energy above an electronic transition excites a molecular vibration with exactly that excess energy as schematically illustrated in Figure 3c.[25,41−43] In d*I*/d*V* spectroscopy in a double-barrier tunnel junction geometry, this results in satellite peaks beyond an electronic resonance with the energy separation of $\hbar\omega$.[21,25,41,42] The intensity ratio of the first replica to the main peak directly gives the dimensionless electron-vibration coupling constant.[41−43]

We will now analyze the line shape and composition of the molecular resonances, concentrating on the corresponding electron lifetimes and the strength of the electron-vibration coupling. Our focus lies on the frontier orbitals of the same symmetry, *i.e.*, the LUMO of the wire CoPC and the HOMO of the pore CoPC. Their

line shape is shown in more detail in the high resolution d*I*/d*V* spectra in Figure 3, panels a and b, respectively. The individual replica have a Lorentzian line shape indicating that the peak width is limited by the lifetime of the molecular resonance and that the intrinsic broadening is small. This is in contrast to the results on alkalihalides, where the molecular resonances have a Gaussian line shape caused by coupling of the tunneling electrons with the optical phonons of the salt.[23,25,44,45] From the measured lifetime, we can estimate the tunneling coupling between a specific molecular orbital and the metallic substrate, which gives us a measure on the insulating properties of h-BN, *i.e.*, how efficiently it decouples the molecules from the Ir(111) surface.

The LUMO of the wire molecule in Figure 3a shows two inelastic peaks in addition to the elastic one. A fit to a sum of three Lorentzian is plotted along with the data and reproduces the line shape of the entire resonance, indicating that lifetime broadening is indeed the dominating process. A confirmation of the vibronic nature of the second and third resonance is given by the linear fit of the peak positions against the peak number as shown in the inset. The slope yields an estimate of the energy of the vibrational mode that couples most strongly with the tunneling electrons, 106 meV. This is in the range of several vibrational modes involving the central cavity of the phthalocyanine,[46] which would be expected to couple strongly with the orbitals centered on the metal.

The HOMO of the pore molecule exhibits even four peaks (see Figure 3b). However, fitting the line shape with a sum of four Lorentzians does not yield as satisfactory agreement with the experimental data as for the LUMO of the wire CoPC. Inspecting the changes of the peak width and area for the extracted individual peaks suggests that the HOMO line shape is a convolution of two close-lying sets of vibronic series. Such an interpretation is supported by the linear fit of the peak position (inset), indicating a slight oscillatory behavior of the energies around the fitted linear dependence. This is reflected in the energy differences (87−128 meV) showing a significantly higher variance than for the wire LUMO (104 − 108 meV).

The first two peaks of the wire LUMO and pore HOMO can be used to estimate the electron-vibration coupling strength.[41−43] This gives roughly 0.8 and 0.4 for the HOMO and LUMO, respectively. This difference might reflect the changes in the electron-vibration coupling constant for the different charge states of the molecule, or the different interaction strengths with the underlying Ir(111) substrate on the wire and the pore. More detailed fitting of the line shape using several vibrational modes will be discussed in the Supporting Information. These fits also give an indication that the HOMO resonance cannot be fully fitted with purely vibronic modes. Finally, we discuss the electron-vibration coupling in the case of the other orbitals (HOMO and LUMO+1) of the wire CoPC in the Supporting Information.

The line width of the elastic peak can be used to estimate the electron lifetime on the molecular resonance. In order to minimize the error in determining the electronic lifetimes due to the asymmetric shape of the elastic peaks caused by coupling to low-energy vibrational modes (Supporting Information), we fit only the leading edge of the wire LUMO and pore HOMO to a single Lorentzian. These fits yield excellent agreement with the experimental onsets of the molecular resonances. We find an average line width of 37 and 60 meV for the wire and pore CoPC, respectively. This indicates that the electronic coupling with the underlying metal substrate is smaller by almost a factor of 2 for the molecules adsorbed in the wire regions of the moiré unit cell, in-line with the weaker bonding between the h-BN and Ir(111) on the wire.

Finally, we want to explore even higher molecular coverages. Figures 4a and b show the sample after deposition of more than one ML of CoPC. Surprisingly, in this regime the adsorption pattern is quite similar to the behavior found at low coverages (Figures 1d,e): the second layer CoPC (marked by a green circle in Figure 4a) adsorbs exclusively on top of the pore molecules of the first layer. Larger scale STM image and a more detailed comparison on the molecular ordering at lower and higher coverages can be found in the Supporting Information. While all the surrounding molecules of the completed first layer exhibit the same bias dependent STM contrasts as below one ML (see Figure 2c), the second layer CoPCs show features of both the wire and the pore molecules. In Figure 4b, it is demonstrated that the central cobalt ion of the second layer CoPC dominates the molecular contrast over a wide bias range. From 2.2 to −1.74 V, the metal center appears as the brightest part of the molecule, indicating its strongly enhanced conductivity. A similar behavior was found previously[47] for second layer CoPC grown on Cu(111). When individual molecules were adsorbed on top sites with respect to the underlying first molecular layer, the polarity dependence of the apparent molecular shape vanished and the cobalt ion showed high conductance at positive and negative bias. DFT calculations revealed that the second layer CoPC forms a dimer with the underlying molecule. Thereby, d_{z^2} and d_{xy} orbitals from the one Co atom hybridize with their corresponding counterparts of the other Co to combine into bonding and antibonding orbitals. In both cases, the bonding orbitals are occupied and the antibonding ones empty, explaining the bright appearance of the second layer CoPC's metal center at positive and negative bias. Thus, we have demonstrated a novel way to assemble CoPC dimers in an ordered array.

Figure 4c displays a d*I*/d*V* spectrum acquired on the metal center of such a dimer formed on top of a h-BN pore. The observed peak structure deviates from the

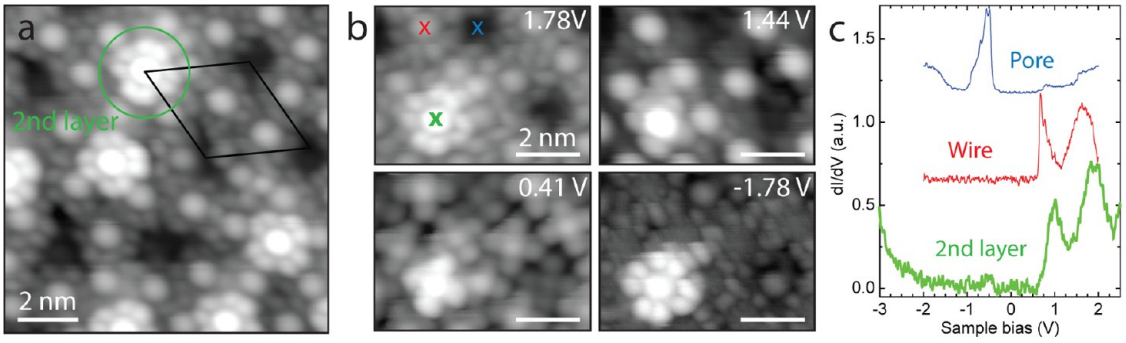

Figure 4. Adsorption of a partial second CoPC layer on h-BN/Ir(111). (a) Large-scale image showing the exclusive adsorption of the second layer CoPC on top of the pore molecules of the first layer. (b) STM images of a second layer CoPC measured at different voltages. (c) d*I*/d*V* spectrum of the second layer molecule (green) marked in (b). Spectra of a pore (blue) and wire (red) molecule measured with the same tip are shown for comparison (spectra are offset for clarity). Feedback parameters: (a) 2.110 V, 12 pA; (b) bias as indicated, set point current is 11 pA for all images.

first layer pore molecules, indicating that the dimer spectrum does not simply correspond to either pore CoPC or to the sum of pore and wire CoPC. On a more general level, the ordered assembly of the second molecular layer on the pore demonstrates a possibility of forming either molecular homo- or heterodimers in a controlled fashion.

CONCLUSIONS

We have shown that monolayers of h-BN grown on a metallic support can act as an ultrathin insulating layer, allowing molecular resonances of adsorbed molecules to be probed. The lifetimes of the tunneling electrons on a molecular resonance are modulated over the moiré superstructure by roughly a factor of 2, due to the different interaction between the molecules and the metal on the pore and on the wire of the h-BN layer. At low coverages, the molecules exclusively adsorb in the pores of the moiré, demonstrating patterned molecular self-assembly on an ultrathin insulating film. Increased coverage results in molecular adsorption also on the wires. Tunneling spectroscopy indicates that the LUMO of the wire CoPC is pushed below the Fermi energy when the molecule is adsorbed on the pore, indicating a local but ordered charging of the molecular layer. This demonstrates the wide range of possibilities to tune not just the ordering but, more importantly, the electronic structure of molecules by controlled deposition on monolayer h-BN on Ir(111). Finally, molecules on the second layer adsorb exclusively on the pore molecules of the first layer making it possible to realize molecular dimers of the same or different phthalocyanines that are spatially ordered and cannot be synthesized by usual chemical means.

METHODS

Sample Preparation. All the experiments were carried out in an ultrahigh vacuum system with a base pressure of $\sim 10^{-10}$ mbar. The (111)-terminated iridium single crystal was cleaned by repeated cycles of sputtering with 1.5 kV neon ions, annealing to 900 °C in 5×10^{-7} mbar oxygen and subsequent flashing to 1400 °C. Full monolayers of h-BN were grown by thermal cracking of borazine ($B_3N_3H_6$, Chemos GmbH) at the Ir(111) substrate held at a temperature of 1160 °C. Subsequently, cobalt phthalocyanine molecules (Sigma-Aldrich) were evaporated from a Knudsen cell at 380 °C onto the h-BN/Ir(111) substrate held at room temperature.

STM Measurements. After the preparation, the sample was inserted into the low-temperature STM (Createc LT-STM) and all subsequent measurements were performed at 5 K. All STM images were acquired in the constant current mode and the images were processed using the WSxM Scanning Probe Microscopy Software.[48] The differential conductance was recorded by lock-in detection on the tunneling current while sweeping the sample bias at constant tip−sample distance; typical parameters for opening the feedback loop were 50 pA tunneling current at 1.8 V sample bias. Voltage modulation during d*I*/d*V* spectroscopy was 20 mV peak-to-peak at a frequency of 517 Hz.

Conflict of Interest: The authors declare no competing financial interest.

Acknowledgment. We thank Ari P. Seitsonen, Mari Ijäs and Ari Harju for discussions. This research made use of the Aalto Nanomicroscopy Center (Aalto NMC) facilities and was supported by the European Research Council (ERC-2011-StG No. 278698 "PRECISE-NANO"), the Academy of Finland (Centre of Excellence in Low Temperature Quantum Phenomena and Devices No. 250280), and the Finnish Academy of Science and Letters.

Supporting Information Available: Additional details on the molecular self-assembly at high surface coverages, and estimating the lifetime of the molecular resonances and fitting of the experimental d*I*/d*V* spectra to a theoretical response based on electron-vibration coupling in a double barrier tunnel junction. This material is available free of charge *via* the Internet at http://pubs.acs.org.

REFERENCES AND NOTES

1. Corso, M.; Auwärter, W.; Muntwiler, M.; Tamai, A.; Greber, T.; Osterwalder, J. Boron Nitride Nanomesh. *Science* **2004**, *303*, 217–220.
2. Corso, M.; Greber, T.; Osterwalder, J. h-BN on Pd(110): A Tunable System for Self-Assembled Nanostructures? *Surf. Sci.* **2005**, *577*, L78–L84.
3. Goriachko, A.; He, Y.; Knapp, M.; Over, H.; Corso, M.; Brugger, T.; Berner, S.; Osterwalder, J.; Greber, T. Self-Assembly of a Hexagonal Boron Nitride Nanomesh on Ru(0001). *Langmuir* **2007**, *23*, 2928–2931.
4. Berner, S.; Corso, M.; Widmer, R.; Groening, O.; Laskowski, R.; Blaha, P.; Schwarz, K.; Goriachko, A.; Over, H.; Gsell, S.;

Schreck, M.; *et al.* Boron Nitride Nanomesh: Functionality from a Corrugated Monolayer. *Angew. Chem., Int. Ed.* **2007**, *46*, 5115–5119.
5. Dil, H.; Lobo-Checa, J.; Laskowski, R.; Blaha, P.; Berner, S.; Osterwalder, J.; Greber, T. Surface Trapping of Atoms and Molecules with Dipole Rings. *Science* **2008**, *319*, 1824–1826.
6. Joshi, S.; Ecija, D.; Koitz, R.; Iannuzzi, M.; Seitsonen, A. P.; Hutter, J.; Sachdev, H.; Vijayaraghavan, S.; Bischoff, F.; Seufert, K.; *et al.* Boron Nitride on Cu(111): An Electronically Corrugated Monolayer. *Nano Lett.* **2012**, *12*, 5821–5828.
7. Gómez Díaz, J.; Ding, Y.; Koitz, R.; Seitsonen, A. P.; Iannuzzi, M.; Hutter, J. Hexagonal Boron Nitride on Transition Metal Surfaces. *Theor. Chem. Acc.* **2013**, *132*, 1350.
8. Vinogradov, N. A.; Zakharov, A. A.; Ng, M. L.; Mikkelsen, A.; Lundgren, E.; Mårtensson, N.; Preobrajenski, A. B. One-Dimensional Corrugation of the h-BN Monolayer on Fe(110). *Langmuir* **2012**, *28*, 1775–1781.
9. Morscher, M.; Corso, M.; Greber, T.; Osterwalder, J. Formation of Single Layer h-BN on Pd(111). *Surf. Sci.* **2006**, *600*, 3280–3284.
10. Preobrajenski, A. B.; Nesterov, M. A.; Ng, M. L.; Vinogradov, A. S.; Mårtensson, N. Monolayer h-BN on Lattice-Mismatched Metal Surfaces: On the Formation of the Nanomesh. *Chem. Phys. Lett.* **2007**, *446*, 119–123.
11. Zunger, A.; Katzir, A.; Halperin, A. Optical Properties of Hexagonal Boron Nitride. *Phys. Rev. B* **1976**, *13*, 5560–5573.
12. Xu, Y.-N.; Ching, W. Y. Calculation of Ground-State and Optical Properties of Boron Nitrides in the Hexagonal, Cubic, and Wurtzite Structures. *Phys. Rev. B* **1991**, *44*, 7787–7798.
13. Rokuta, E.; Hasegawa, Y.; Suzuki, K.; Gamou, Y.; Oshima, C.; Nagashima, A. Phonon Dispersion of an Epitaxial Monolayer Film of Hexagonal Boron Nitride on Ni(111). *Phys. Rev. Lett.* **1997**, *79*, 4609–4612.
14. Laskowski, R.; Blaha, P.; Schwarz, K. Bonding of Hexagonal BN to Transition Metal Surfaces: An *ab Initio* Density-Functional Theory Study. *Phys. Rev. B* **2008**, *78*, 045409.
15. Preobrajenski, A. B.; Krasnikov, S. A.; Vinogradov, A. S.; Ng, M. L.; Käämbre, T.; Cafolla, A. A.; Mårtensson, N. Adsorption-Induced Gap States of *h*-BN on Metal Surfaces. *Phys. Rev. B* **2008**, *77*, 085421.
16. Bose, S.; García-García, A. M.; Ugeda, M. M.; Urbina, J. D.; Michaelis, C. H.; Brihuega, I.; Kern, K. Observation of Shell Effects in Superconducting Nanoparticles of Sn. *Nat. Mater.* **2010**, *9*, 550–554.
17. Kahle, S.; Deng, Z.; Malinowski, N.; Tonnoir, C.; Forment-Aliaga, A.; Thontasen, N.; Rinke, G.; Le, D.; Turkowski, V.; Rahman, T. S.; *et al.* The Quantum Magnetism of Individual Manganese-12-Acetate Molecular Magnets Anchored at Surfaces. *Nano Lett.* **2012**, *12*, 518–521.
18. Nilius, N.; Ernst, N.; Freund, H.-J. Photon Emission Spectroscopy of Individual Oxide-Supported Silver Clusters in a Scanning Tunneling Microscope. *Phys. Rev. Lett.* **2000**, *84*, 3994–3997.
19. Qiu, X. H.; Nazin, G. V.; Ho, W. Vibrationally Resolved Fluorescence Excited with Submolecular Precision. *Science* **2003**, *299*, 542–546.
20. Heinrich, A. J.; Gupta, J. A.; Lutz, C. P.; Eigler, D. M. Single-Atom Spin-Flip Spectroscopy. *Science* **2004**, *306*, 466–469.
21. Qiu, X. H.; Nazin, G. V.; Ho, W. Vibronic States in Single Molecule Electron Transport. *Phys. Rev. Lett.* **2004**, *92*, 206102.
22. Repp, J.; Meyer, G.; Olsson, F. E.; Persson, M. Controlling the Charge State of Individual Gold Adatoms. *Science* **2004**, *305*, 493–495.
23. Repp, J.; Meyer, G.; Stojković, S. M.; Gourdon, A.; Joachim, C. Molecules on Insulating Films: Scanning-Tunneling Microscopy Imaging of Individual Molecular Orbitals. *Phys. Rev. Lett.* **2005**, *94*, 026803.
24. Liljeroth, P.; Repp, J.; Meyer, G. Current-Induced Hydrogen Tautomerization and Conductance Switching of Naphthalocyanine Molecules. *Science* **2007**, *317*, 1203–1206.
25. Repp, J.; Liljeroth, P.; Meyer, G. Coherent Electron-Nuclear Coupling in Oligothiophene Molecular Wires. *Nat. Phys.* **2010**, *6*, 975–979.
26. Wu, S. W.; Ogawa, N.; Ho, W. Atomic-Scale Coupling of Photons to Single-Molecule Junctions. *Science* **2006**, *312*, 1362–1365.
27. Wu, S. W.; Ogawa, N.; Nazin, G. V.; Ho, W. Conductance Hysteresis and Switching in a Single-Molecule Junction. *J. Phys. Chem. C* **2008**, *112*, 5241–5244.
28. Swart, I.; Sonnleitner, T.; Repp, J. Charge State Control of Molecules Reveals Modification of the Tunneling Barrier with Intramolecular Contrast. *Nano Lett.* **2011**, *11*, 1580–1584.
29. Ma, H.; Brugger, T.; Berner, S.; Ding, Y.; Iannuzzi, M.; Hutter, J.; Osterwalder, J.; Greber, T. Nano-Ice on Boron Nitride Nanomesh: Accessing Proton Disorder. *ChemPhysChem* **2010**, *11*, 399–403.
30. Orlando, F.; Larciprete, R.; Lacovig, P.; Boscarato, I.; Baraldi, A.; Lizzit, S. Epitaxial Growth of Hexagonal Boron Nitride on Ir(111). *J. Phys. Chem. C* **2012**, *116*, 157–164.
31. Schulz, F.; Drost, R.; Hämäläinen, S. K.; Demonchaux, T.; Seitsonen, A. P.; Liljeroth, P. The Structure of Hexagonal Boron Nitride on Ir(111). Unpublished work, **2013**.
32. Lu, X.; Hipps, K. W.; Wang, X. D.; Mazur, U. Scanning Tunneling Microscopy of Metal Phthalocyanines: d^7 and d^9 Cases. *J. Am. Chem. Soc.* **1996**, *118*, 7197–7202.
33. Hipps, K. W.; Lu, X.; Wang, X. D.; Mazur, U. Metal d-Orbital Occupation-Dependent Images in the Scanning Tunneling Microscopy of Metal Phthalocyanines. *J. Phys. Chem.* **1996**, *100*, 11207–11210.
34. Zhao, A.; Li, Q.; Chen, L.; Xiang, H.; Wang, W.; Pan, S.; Wang, B.; Xiao, X.; Yang, J.; Hou, J. G.; *et al.* Controlling the Kondo Effect of an Adsorbed Magnetic Ion through Its Chemical Bonding. *Science* **2005**, *309*, 1542–1544.
35. Chen, L.; Hu, Z.; Zhao, A.; Wang, B.; Luo, Y.; Yang, J.; Hou, J. G. Mechanism for Negative Differential Resistance in Molecular Electronic Devices: Local Orbital Symmetry Matching. *Phys. Rev. Lett.* **2007**, *99*, 146803.
36. Hu, Z.; Chen, L.; Zhao, A.; Li, Z.; Wang, B.; Yang, J.; Hou, J. G. Detecting a Molecule-Surface Hybrid State by an Fe-Coated Tip with a Non-s-Like Orbital. *J. Phys. Chem. C* **2008**, *112*, 15603–15606.
37. Iacovita, C.; Rastei, M. V.; Heinrich, B. W.; Brumme, T.; Kortus, J.; Limot, L.; Bucher, J. P. Visualizing the Spin of Individual Cobalt-Phthalocyanine Molecules. *Phys. Rev. Lett.* **2008**, *101*, 116602.
38. Järvinen, P.; Hämäläinen, S. K.; Banerjee, K.; Häkkinen, P.; Ijäs, M.; Harju, A.; Liljeroth, P. Molecular Self-Assembly on Graphene on SiO_2 and h-BN Substrates. *Nano Lett.* **2013**, *13*, 3199–3204.
39. Olsson, F. E.; Paavilainen, S.; Persson, M.; Repp, J.; Meyer, G. Multiple Charge States of Ag Atoms on Ultrathin NaCl Films. *Phys. Rev. Lett.* **2007**, *98*, 176803.
40. Lu, X.; Grobis, M.; Khoo, K. H.; Louie, S. G.; Crommie, M. F. Charge Transfer and Screening in Individual C_{60} Molecules on Metal Substrates: A Scanning Tunneling Spectrocsopy and Theoretical Study. *Phys. Rev. B* **2004**, *70*, 115418.
41. Wingreen, N. S.; Jacobsen, K. W.; Wilkins, J. W. Resonant Tunneling with Electron-Phonon Interaction: An Exactly Solvable Model. *Phys. Rev. Lett.* **1988**, *61*, 1396–1399.
42. Wingreen, N. S.; Jacobsen, K. W.; Wilkins, J. W. Inelastic Scattering in Resonant Tunneling. *Phys. Rev. B* **1989**, *40*, 11834–11850.
43. Gadzuk, J. W. Inelastic Resonance Scattering, Tunneling, and Desorption. *Phys. Rev. B* **1991**, *44*, 13466–13477.
44. Repp, J.; Meyer, G.; Paavilainen, S.; Olsson, F. E.; Persson, M. Scanning Tunneling Spectroscopy of Cl Vacancies in NaCl Films: Strong Electron-Phonon Coupling in Double-Barrier Tunneling Junctions. *Phys. Rev. Lett.* **2005**, *95*, 225503.
45. Pavliček, N.; Swart, I.; Niedenführ, J.; Meyer, G.; Repp, J. Symmetry Dependence of Vibration-Assisted Tunneling. *Phys. Rev. Lett.* **2013**, *110*, 136101.
46. Liu, Z.; Zhang, X.; Zhang, Y.; Jiang, J. Theoretical Investigation of the Molecular, Electronic Structures and Vibrational Spectra of a Series of First Transition Metal Phthalocyanines. *Spectrochim. Acta, Part A* **2007**, *67*, 1232–1246.

47. Ge, X.; Manzano, C.; Berndt, R.; Anger, L. T.; Köhler, F.; Herges, R. Controlled Formation of an Axially Bonded Co-Phthalocyanine Dimer. *J. Am. Chem. Soc.* **2009**, *131*, 6096–6098.
48. Horcas, I.; Fernandez, R.; Gomez-Rodriguez, J. M.; Colchero, J.; Gomez-Herrero, J.; Baro, A. M. WSXM: A Software for Scanning Probe Microscopy and a Tool for Nanotechnology. *Rev. Sci. Instrum.* **2007**, *78*, 013705.